Supporting Information: *In situ* structure and dynamics of DNA origami determined through molecular dynamics simulations

Jejoong Yoo * **and Aleksei Aksimentiev** * †

*Department of Physics and Center for the Physics of Living cells, University of Illinois at Urbana–Champaign, 1110 West Green Street, Urbana, Illinois 61801, and †Beckman Institute for Advanced Science and Technology

Submitted to Proceedings of the National Academy of Sciences of the United States of America

Design and simulation of the DNA origami structures

To obtain fully atomistic models of DNA origami objects, we designed the target DNA origami structures using the caDNAno software, converted the caDNAno designs into all-atom representations and refined the all-atom structures by performing MD simulations.

Design of the DNA origami structures. Using caDNAno, we designed the following three DNA origami structures: a straight 6-by-3 honeycomb-pleated structure (HC), a straight 4-by-4 square-pleated structure (SQ), and a 6-by-3 honeycomb-pleated structure having a 90° programmable bend (HC-90°). Below, we briefly describe our protocols for obtaining the caDNAno designs.

Building a DNA origami structure in caDNAno begins with sketching the overall shape of the target structure using cylinders. Fig. S1A illustrates this step for the HC structure. The cylinders (numbered by index m) depict the volumes where fragments of duplex DNA will be placed; the blue and red tubes represent the backbone traces of the DNA strands. In the target structure, neighboring cylinders ($m = i, i + 1$) are connected to each other, forming a single sheet that includes all cylinders. The particular three-dimensional (3D) fold of the sheet is obtained by introducing additional connections between the cylinders, for example, between $m = 2$ and $m = 11$ in Fig. S1A. In the final structure, all cylinders are arranged parallel to one another and form either a honeycomb or square lattice pattern within the plane normal to the axes of the cylinders. For convenience, we define the z-axis to be parallel to the axes of the cylinders.

Next, we determine the length, sequence and spatial arrangement of the DNA strands that can realize the cylinder model. At this stage of the process, it is convenient to represent the DNA origami object as a two-dimensional (2D) sheet. Fig. S1B, Fig. S2A, and Fig. S2B show 2D schematics of our HC, SQ and HC-90° objects, respectively. A long scaffold strand is manually designed to span the entire 2D sheet, crossing over between neighboring cylinders [1]. The caDNAno program generates a collection of short (usually 18 to 49 nucleotide-long) staple strands that, together with the scaffold strand, form duplex DNA. The nucleotide sequence of the staples uniquely will define their positions along the scaffold. In a 3D DNA origami structure, a staple strand can form a crossover between either two neighboring or two distant (within the 2D sheet) DNA helixes.

Because duplex DNA has a helical pitch, staple crossovers can be realized only at specific locations in a periodic 3D origami structure. The caDNAno software places the staple crossovers at designated crossover planes. For the HC object, the crossover planes are depicted as semi-transparent rectangles in Fig. S1A and as gray columns in Fig. S1B. The location of the crossover planes depends on the type of the DNA lattice. In a honeycomb lattice, each cylinder has three nearest neighbors and the DNA helix rotates by 240°between two consecutive crossover planes (by 270°in a square lattice where each cylinder has four nearest neighbors). A 240°or 270°rotation of a B-form DNA helix is equivalent to an axial displacement by 7 or 8 base pairs, respectively. Thus, the crossover planes occur periodically and the structures repeat themselves every 3 or 4 crossover planes (21 or 32 base pairs) in the honeycomb or square lattice, respectively. Two neighboring crossover planes define an array cell. Each array cell contains 7 or 8 base pairs per cylinder in the honeycomb or square lattice, respectively [2], Fig. S1B. The scaffold crossovers can occur outside the staple crossover planes. For a large 3D DNA origami object, the majority of connections between the cylinders is realized by staple crossovers. The distributions of scaffold and staple crossovers in our designs of DNA origami objects are shown at the bottom of Fig. S1B, and Fig. S2A,B.

In the final step, the scaffold strand is assigned a nucleotide sequence of a fragment of the M13 viral genome. The nucleotide sequence of the staple strands is chosen to complement the sequence of the scaffold strand. The sequence assignment is automated by the caDNAno program.

Conversion of caDNAno design to all-atom representation. We constructed an all-atom model from a caDNAno design in the following three steps. First, we built all-atom template models of the four possible base pairs that a scaffold and a staple strand can form in our structures: dA·dT, dT·dA, dG·dC, and dC·dG. The center of mass (CoM) of the four template models were placed at the origin of our coordinate system. The base pairs were oriented to have the vector connecting the CoM of the sugar group of the scaffold strand to the CoM of the sugar group of the staple strand parallel to x-axis. Second, the atomic coordinates of a base pair of base index i_z in cylinder m were determined by rotating the corresponding template structure by $i_z\Delta\theta + \theta_0$ about the z-axis and translating the coordinates by $(x_m^{\mathrm{CoM}}, y_m^{\mathrm{CoM}}, i_z\Delta z)$, where $\Delta\theta = 360°/10.5$ and $\Delta z = 3.4$ Å are the turn and the rise per base pair of B-DNA, respectively. In the above description, x_m^{CoM} and y_m^{CoM} are $x-$ and $y-$coordinates of the center of cylinder m. The constant factor θ_0 was chosen to align the base pairs within the crossover planes with the coordinate system, see Fig. S1C–E. The distance between the axes of two neighboring DNA duplexes was set to 2 nm. Last, the DNA nucleotides forming the scaffold and staple strands were connected to form continuous DNA strands using the connectivity information from caDNAno. The entire process was automated by a homemade perl script that converted the outputs files from caDNAno into a PDB format. The script and the PDB format atomistic structures are available upon request. The caDNAno designs and the corresponding pdb models of our HC, SQ, and HC-90° systems are available as Supporting Information files.

Reserved for Publication Footnotes

Multi-step equilibration of the HC-90°structure. First, we equilibrated the HC-90°system for 2 ns applying harmonic constraints ($k = 1$ kcal/mol/Å^2) to all heavy atoms of DNA bases in a relatively small water box ($\sim 14 \times 15 \times 60$ nm^3). During this step, Mg^{2+} ions redistributed within the origami, Fig. S3A,B. Following that, the water box size was increased to $\sim 26 \times 18 \times 60$ nm^3 by adding pre-equilibrated 10 mM solution of $MgCl_2$, Fig. S3C. To allow the helices carrying insertions or deletions to expand or shrinking while maintaining the local structural order, we used harmonic distance restraints between all pairs of heavy atoms of DNA bases located within a 10 Å cutoff, Fig. S3 and Animation M7. Under such distance restraints, the system was equilibrated for 1 ns with the spring constant of 0.4 kcal/mol/Å^2, resulting in a slight bending of the structure, Fig. S3C. The simulation was continued for 1.6 ns with $k = 0.05$ kcal/mol/Å^2, which increased bending of the structure Fig. S3D,E. At the end of the equilibration, HC-90° system formed a bending angle of ∼90°, Fig. S3E. The final conformations of the equilibration simulations were used for production runs.

All-atom simulations using the AMBER99bsc0 force field. We also simulated our three DNA origami structures using the AMBER99bsc0 DNA force field [3] in combination with the original TIP3P water model [4] and ion parameters developed by Jeon et al. [5] and improved by Yoo et al. [6]. These simulations (summarized in Table S1) were performed using the Gromacs package [7]. For our AMBER99bsc0 simulations, we used the same initial conformations, the same simulation parameters, and the same equilibration procedures as for our simulations that employed the CHARMM36 force field. Specifically, the temperature was kept constant at 298 K using the Nosé-Hoover scheme [8, 9]. The pressure was kept constant at 1 bar using the Parrinello-Rahman scheme [10]. The grid size for the Particle-Mesh Ewald summation was 1.2 Å [11].

The results of the AMBER99bsc0 simulations were considerably different from the results obtained using the CHARMM36 force field. When simulated using the AMBER99bsc0 force field, the honeycomb-based structures developed significant twists ($\omega_3 = 2 - 4°$/cell) that were absent in our CHARMM36 simulations. Such twists are inconsistent with experimental measurements [1], Fig. S10G,I. Furthermore, the overall bending angle of the HC-90° structure converged to ∼120° in our AMBER99bsc0 simulations, which is also inconsistent with the experimentally determined angle of ∼90° [1], Fig. S10E,F. Thus, we found all-atom simulations of DNA origami structures using the AMBER99bsc0 force field to exhibit considerable artifacts. Such artifacts were absent in analogous simulations performed using CHARMM36.

Definition of triad vectors

For our calculations of mechanical properties of monolith-like structures, it was natural to define a contour, $s = 0, \ldots, L$, parallel to the central axis of each cylinder. Specifically, the contour was defined as a line that connects the CoMs of the neighboring array cells, Fig. 5A. For each array cell, we also defined a least-squares plane that minimizes the sum of distances to the CoMs of DNA in the same-index cells. In Fig. 5A, the least-squares planes are shown in gray. Then, we defined a triad of unit vectors, $\{\hat{t}_i(s)|i = 1, 2, 3\}$, that were fixed in each array-cell plane (Fig. 4A inset). For the 6-by-3 honeycomb structure, $\hat{t}_1$ was parallel to the line connecting helix 7 and 11, whereas $\hat{t}_3$ was normal to the plane and $\hat{t}_2 = \hat{t}_3 \times \hat{t}_1$.

Animations of MD trajectories

Animation M1: HC-hbonds-layer1.mpg. This animation illustrates the dynamics of base pairing at the single nucleotide level for the first layer ($m = 1 \cdots 6$) of the HC structure during the ∼130-ns production simulation. The backbone and bases of DNA are shown as tubes; each DNA strand has a unique color. Base pairs from the non-peripheral region of the structure that remained broken for 10 ns or more are highlighted using the vdW (spheres) representations. In frame zero, the circle indicates a base pair from array cell 6 that breaks and reforms during the simulation.

Animation M2: HC-hbonds-layer2.mpg. Same as Animation M1 showing the second layer ($m = 7 \cdots 12$) of the HC structure.

Animation M3: HC-hbonds-layer3.mpg. Same as Animation M1 showing the third layer ($m = 13 \cdots 18$) of the HC structure.

Animation M4: HC.mov. This animation illustrates the production simulation of the HC structure, covering ∼130 ns. The DNA origami structure is shown using a custom color-coded chicken wire representation. The wire frame (black lines) connects the CoMs of the DNA base pairs that form continuous double-stranded DNA cylinders of the original DNA origami designs. The lines between the CoMs of the same-index base pairs connect the wire frame. The length of the lines indicate the local inter-DNA distance, which is color-coded.

Animation M5: SQ.mov. This animation illustrates the production simulation of the SQ structure, covering ∼120 ns. The DNA origami structure is shown using a custom color-coded chicken wire representation as described for Animation 4.

Animation M6: HC90.mov. This animation illustrates the production simulation of the HC-90° structure, covering ∼30 ns. The DNA origami structure is shown using a custom color-coded chicken wire representation as described for Animation M4.

Animation M7: HC90-equil.mov. This animation illustrates the equilibration process that allows 90° bending of the HC-90° structure.

1. Dietz H, Douglas SM, Shih WM (2009) Folding DNA into twisted and curved nanoscale shapes. *Science* 325(5941):725–30.
2. Douglas SM, et al. (2009) Rapid prototyping of 3D DNA-origami shapes with caDNAno. *Nucl Acids Res* 37(15):5001–6.
3. Perez A, et al. (2007) Refinement of the AMBER force field for nucleic acids: Improving the description of α/γ conformers. *Biophys J* 92:3817–3829.
4. Jorgensen WL, Chandrasekhar J, Madura JD, Impey RW, Klein ML (1983) Comparison of simple potential functions for simulating liquid water. *J Chem Phys* 79(2):926–935.
5. Joung I, Cheatham T (2009) Molecular dynamics simulations of the dynamic and energetic properties of alkali and halide ions using water-model-specific ion parameters. *J Phys Chem B* 113(40):13279–90.
6. Yoo J, Aksimentiev A (2012) Improved parametrization of Li^+, Na^+, K^+, and Mg^{2+} ions for all-atom molecular dynamics simulations of nucleic acid systems. *J Phys Chem Lett* 3(1):45–50.
7. Hess B, Kutzner C, Van Der Spoel D, Lindahl E (2008) Gromacs 4: Algorithms for highly efficient, load-balanced, and scalable molecular simulation. *J Chem Theory Comput* 4(3):435–447.
8. Nose S, Klein ML (1983) Constant pressure molecular dynamics for molecular systems. *Mol Phys* 50:1055–76.
9. Hoover WG (1985) Canonical dynamics: Equilibrium phase-space distributions. *Phys Rev A* 31(3):1695–1697.
10. Parrinello M, Rahman A (1981) Polymorphic transitions in single crystals: A new molecular dynamics method. *J Appl Phys* 52(12):7182–90.
11. Darden T, York D, Pedersen L (1993) Particle mesh ewald: An n log(n) method for ewald sums in large systems. *J Chem Phys* 98(12):10089–92.

Table S1. Production MD simulations of DNA origami objects.

System	# Array cell	# Cylinder	# nucleotides	# atoms	# staples	Simulation Time (ns)	
						CHARMM	AMBER
HC	11	$6 \times 3 = 18$	2,640	802,149	43	$\sim$140	$\sim$100
HC-90°	27	$6 \times 3 = 18$	6,420	2,799,156	87	$\sim$30	$\sim$30
SQ	16	$4 \times 4 = 16$	3,760	943,837	55	$\sim$120	$\sim$100

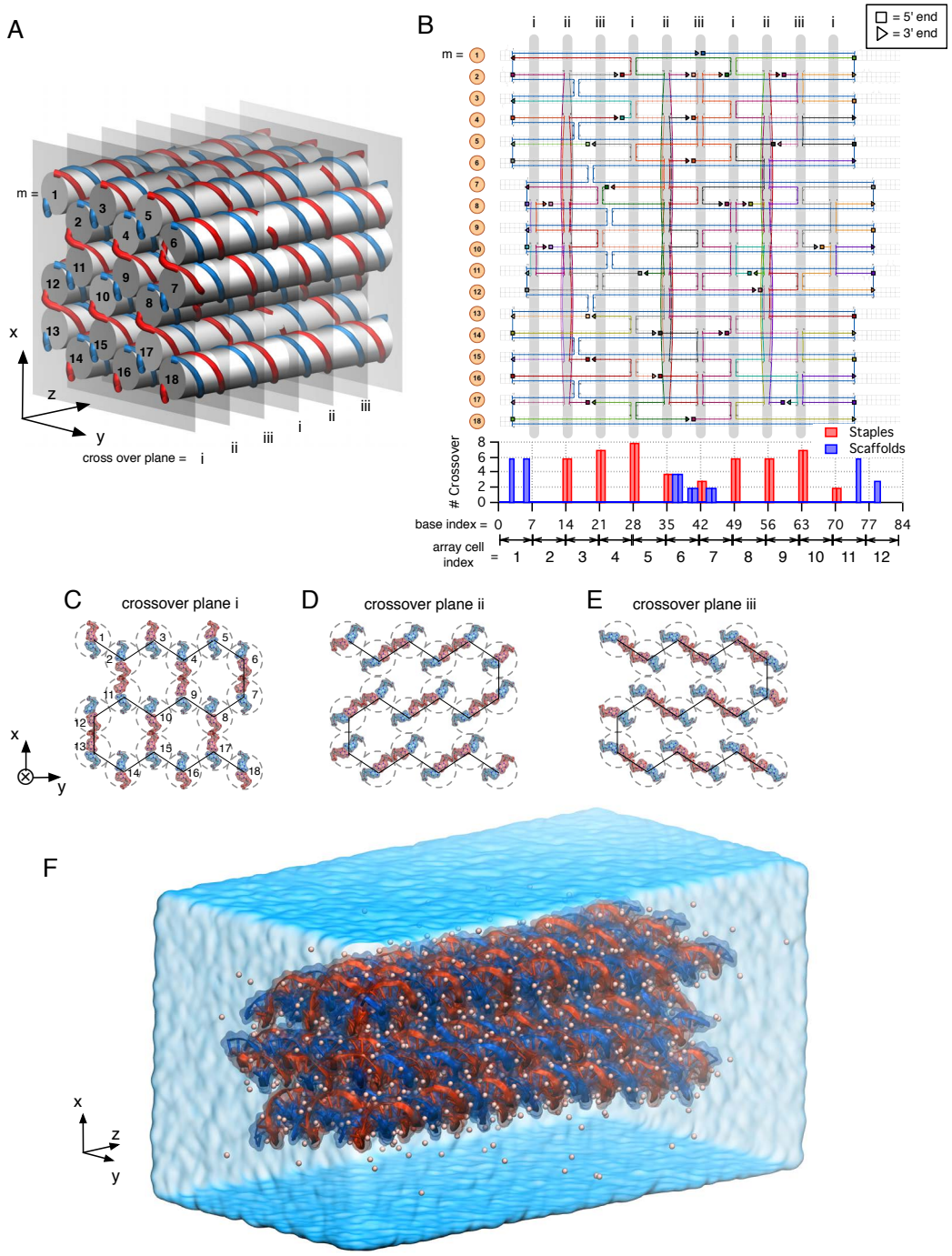

Fig. S1. Construction of all-atom origami structure using the caDNAno design. (A) A 3D cartoon view of the 6-by-3 honeycomb-pleated origami design (HC). Cylinders ($m = 1, \cdots, 18$) depict how DNA duplexes are organized into a 3D structure. For convenience, the DNA duplexes are aligned with the z-axis. Blue and red tubes illustrate the backbone traces of the cylinder-filling DNA strands. In this particular structure, six consecutive helices form one layer ($m = 1, \cdots, 6, m = 7, \cdots, 12$, and $m = 13, \cdots, 18$); the three DNA layers fold into a multi-layer structure. In our SQ structure (not shown), four helices form one layer and four layers form a 4-by-4 square-pleated structure. (B) *Top*. A 2D schematic view of the paths the DNA strands form within the HC structure. The long blue path covering the entire space represents the scaffold DNA strand; all other short paths represent the staple strands [1]. In panel A, the scaffold and staple strands are represented by the blue and red tubes, respectively. The scaffold and staple paths cross over between cylinders at designated crossover planes. The crossover planes for staple strands are depicted as semi-transparent gray planes and vertical gray lines in panels A and B, respectively. *Bottom*. The number of crossovers as a function of base index for the HC system. (C–E) Atomistic representations of the HC structure at the three unique crossover planes for staple strands. The nucleotides forming the scaffold and staple strands are shown in blue and red, respectively. (F) The final all-atom model of the HC system in an aqueous environment. The scaffold and staple strands are shown in blue and red molecular graphics representations, respectively. Mg^{2+} ions are shown as pink spheres; the water box is drawn as a semi-transparent blue surface.

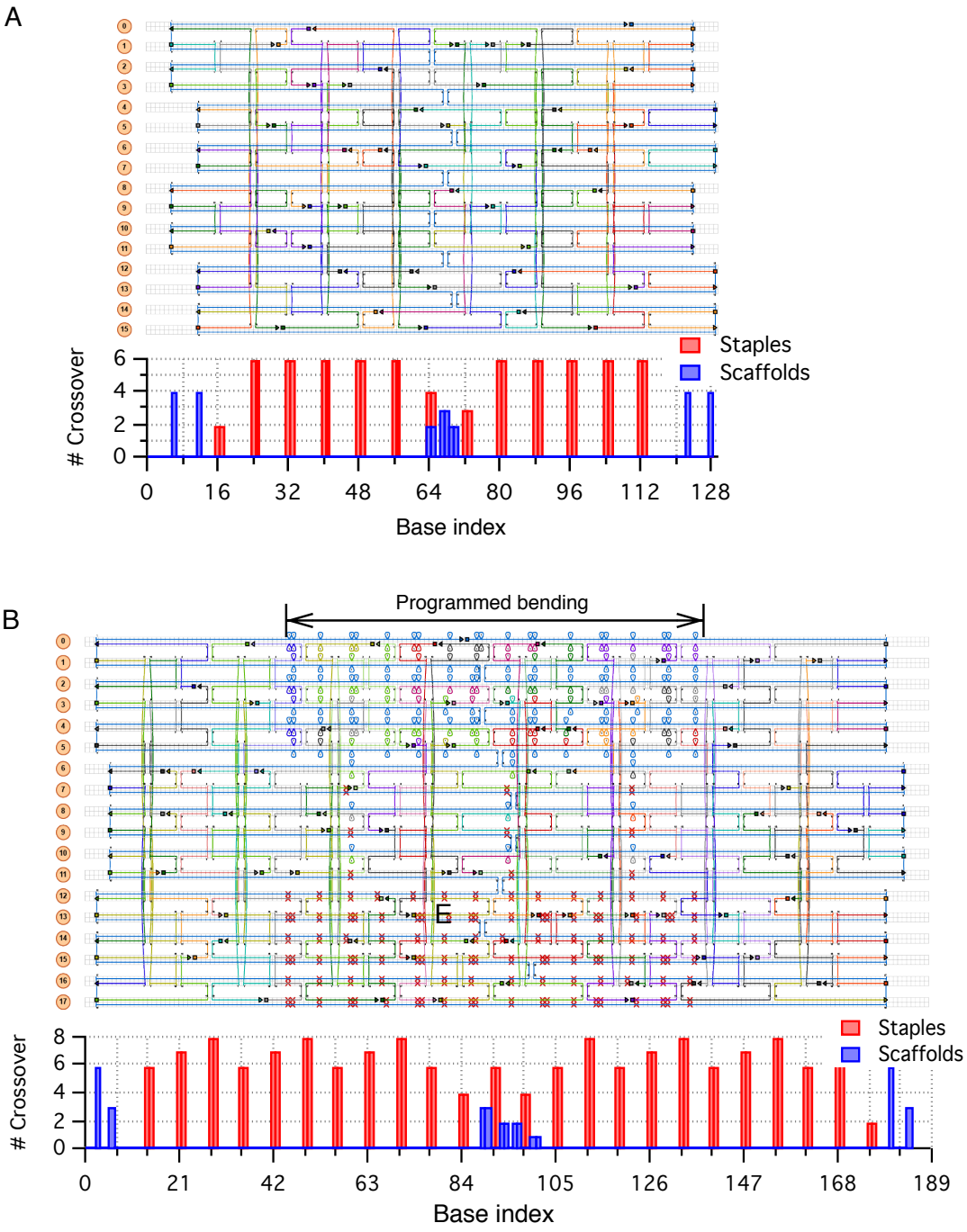

Fig. S2. 2D caDNAno designs of the 4-by-4 square-pleated origami structure, SQ panel A, and of the 6-by-3 honeycomb-pleated origami having a 90° bent, HC-90° panel B. The long blue paths represent the scaffold DNA strands whereas the short paths of other colors represent the staple strands. The loops and crosses in panel B indicate insertions and deletions, respectively. At the bottom of each panel, the number of scaffold (blue bars) and staple (red bars) crossovers is shown as a function of base index.

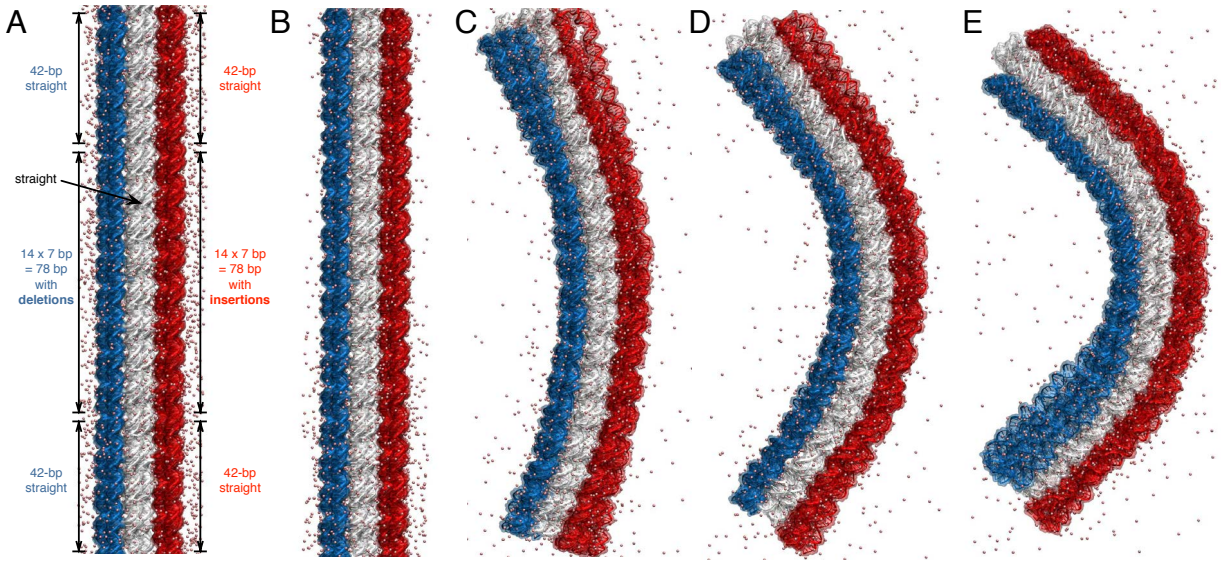

Fig. S3. Equilibration of the HC-90° system. (A) Initial all-atom structure constructed by converting the caDNAno design (see Figure S1) to all-atom coordinates. The three different layers of the structure ($m = 1, \cdots, 6$, $m = 7, \cdots, 12$, and $m = 13, \cdots, 18$ helices) are shown in red, white, and blue. Randomly placed Mg^{2+} ions are shown as spheres. (B) First 2 ns of equilibration: all non-hydrogen atoms of DNA bases are restrained to their initial coordinates; Mg^{2+} ions migrate to their equilibrium locations within the DNA origami structure. (C-E) A bend in the structure is produced by allowing the DNA helices to expand and shrink according to the insertions and deletions introduced in the design, Fig. S2B. To preserve the local order of the structure, the distance between non-hydrogen atoms of the DNA bases within 10 Å was restrained. Such elastic-network-like restraints were realized by introducing harmonic bonds using the extra bonds feature of NAMD. Then, the restraints were removed in steps. In the first step, the system was equilibrated for 1 ns having the spring constant of the distance restraints set to 0.4 kcal/mol/Å^2; the DNA origami developed a slight bend (C). During subsequent 1.6-ns equilibration with a smaller force constant (0.05 kcal/mol/Å^2), a bend of approximately 90° fully developed (D,E). Animation M7 illustrates the equilibration process.

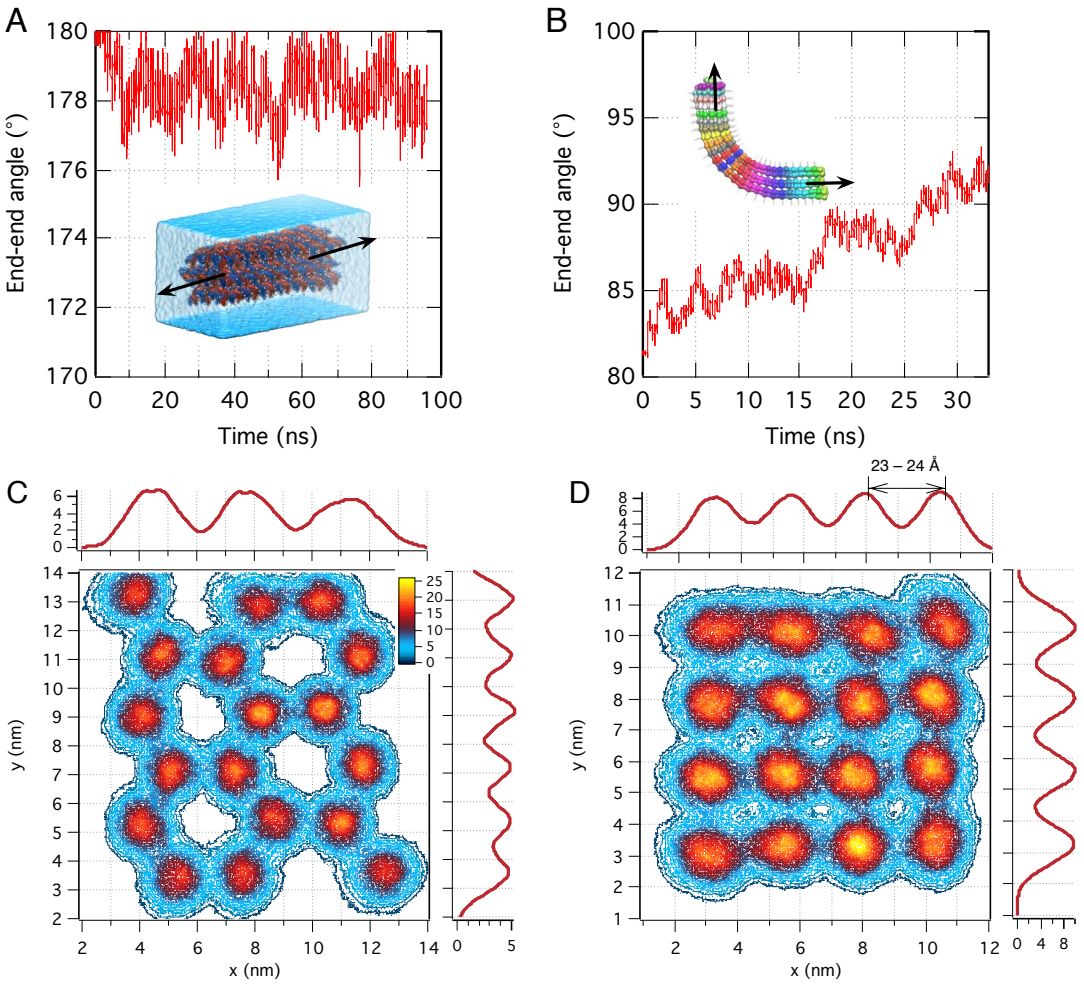

Fig. S4. Global conformation of DNA origami objects. (A,B) The angle between the tangential vectors at the ends of the HC (A) and HC-90° (B) objects as a function of simulation time. The tangential vectors (parallel to the central contour line) at the ends of the structures are illustrated using black arrows. (C,D) 2D density maps of the central regions of the HC (C) and SQ (D) objects. The maps illustrate the average arrangement of DNA helices within the plane normal to the cylinders' axes. To produce the 2D maps, the number density of non-hydrogen DNA base atoms were first computed over a 3D cubic grid at 0.2 Å resolution. The 3D density maps were averaged over 10- (C) or 20- (D) nm central region of the respective object. Plots at the top and right sides of panel C and D show the DNA density profiles computed by averaging the 2D maps over $y-$ or $x-$ axis, respectively. Data shown in panels C and D were averaged over the last 60 ns of the respective MD trajectories.

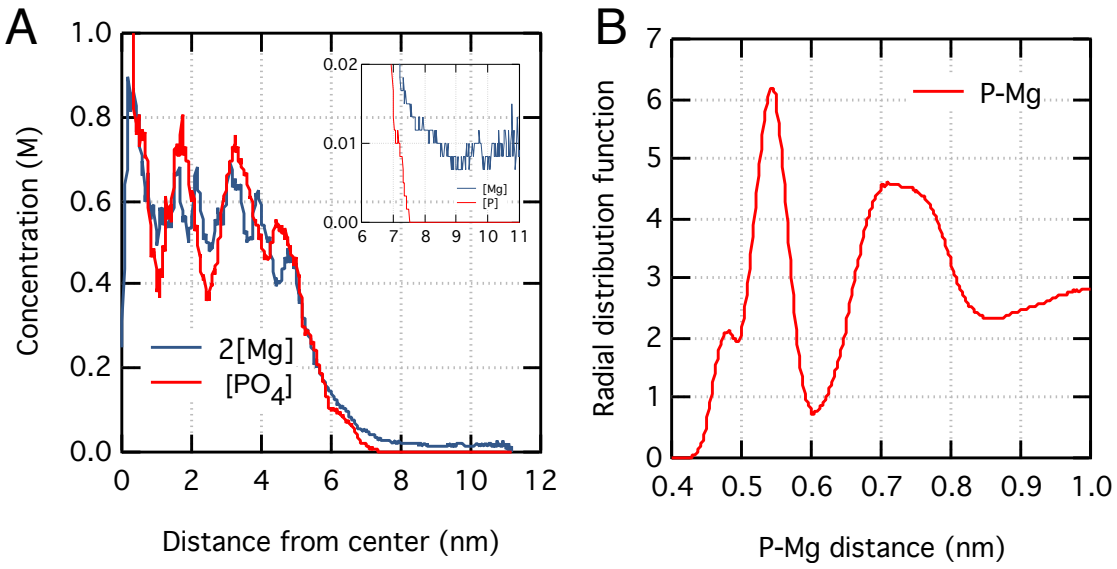

Fig. S5. Distribution of magnesium ions in HC DNA origami. (A) Concentrations of Mg^{2+} and phosphate versus distance from the central axis of the HC system. The inset shows a close-up view of the graph. The charge of Mg^{2+} ions cancels the charge of DNA inside the DNA origami object. The concentration of Mg^{2+} outside DNA origami is 10 mM (see Inset). (B) Radial distribution function of Mg^{2+} with respect to the phosphorus atom of DNA backbone. Data in panels A and B were obtained by averaging over the last 60 ns of the HC system's trajectory.

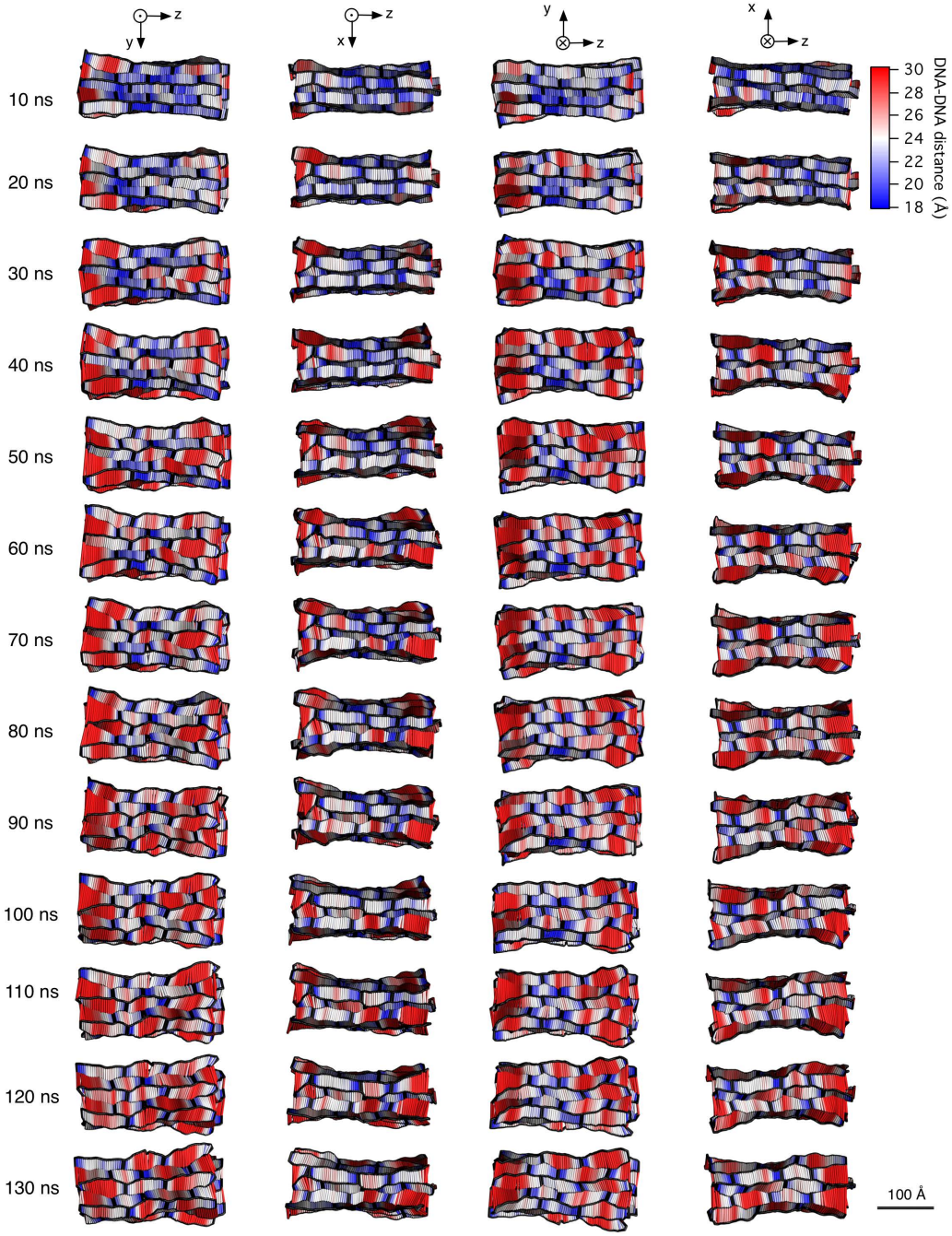

Fig. S6. Snapshots illustrating the MD trajectory of the HC system. The DNA origami structure is shown using a custom color-coded chicken wire representation. The wire frame (black lines) connect the centers of mass of the DNA base pairs that form continuous double-stranded DNA cylinders or crossovers of the original DNA origami designs. The lines between the centers of mass of the same-index base pairs connect the wire frame. The length of the lines indicate the local inter-DNA distance, which is color-coded. The same system is shown from four different view points (same for each column). Animation M4 illustrates this MD trajectory.

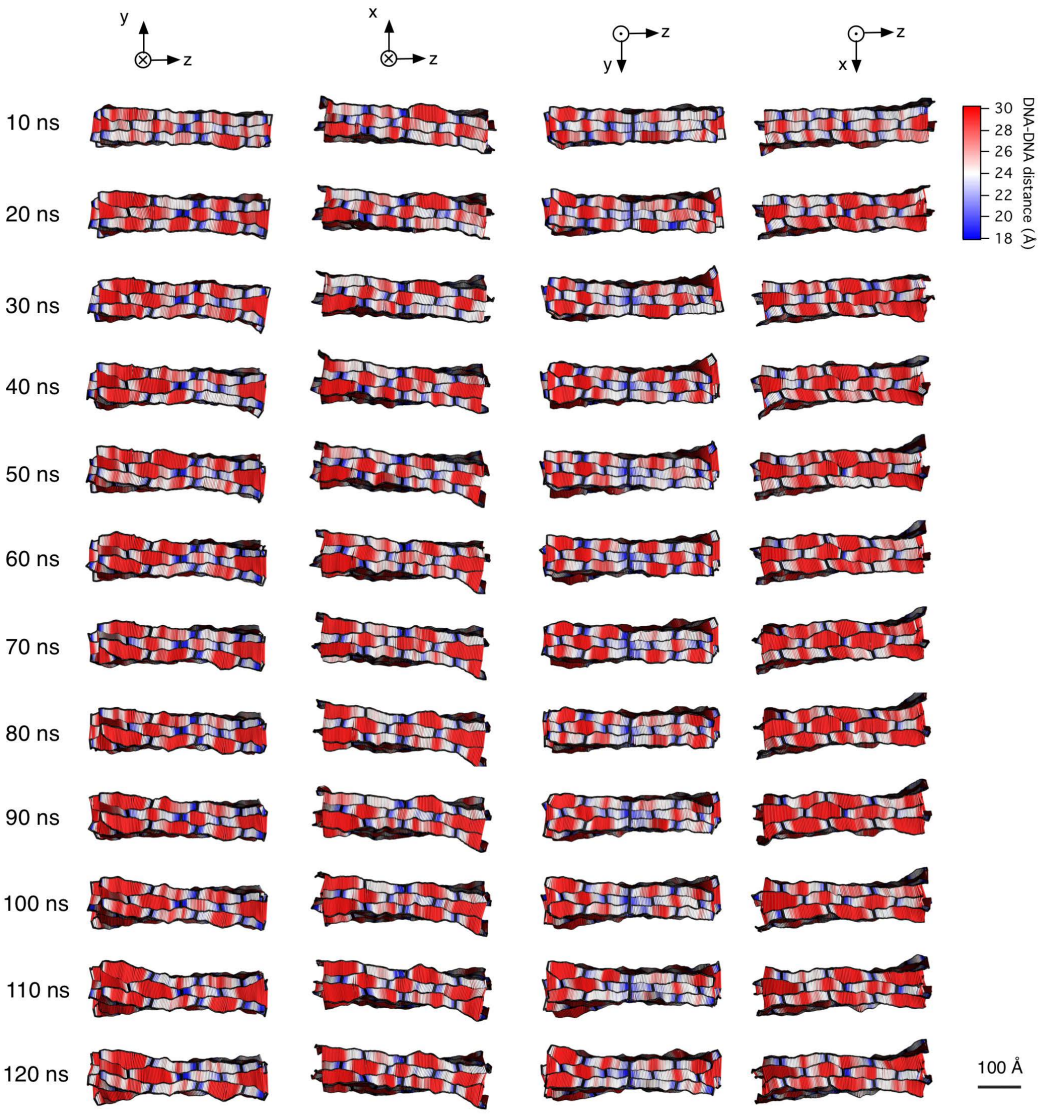

Fig. S7. Snapshots illustrating the MD trajectory of the SQ system. The DNA origami structure is shown using a custom color-coded chicken wire representation. The wire frame (black lines) connect the centers of mass of the DNA base pairs that form continuous double-stranded DNA cylinders or crossovers of the original DNA origami designs. The lines between the centers of mass of the same-index base pairs connect the wire frame. The length of the lines indicate the local inter-DNA distance, which is color-coded. The same system is shown from four different view points (same for each column). Animation M5 illustrates this MD trajectory.

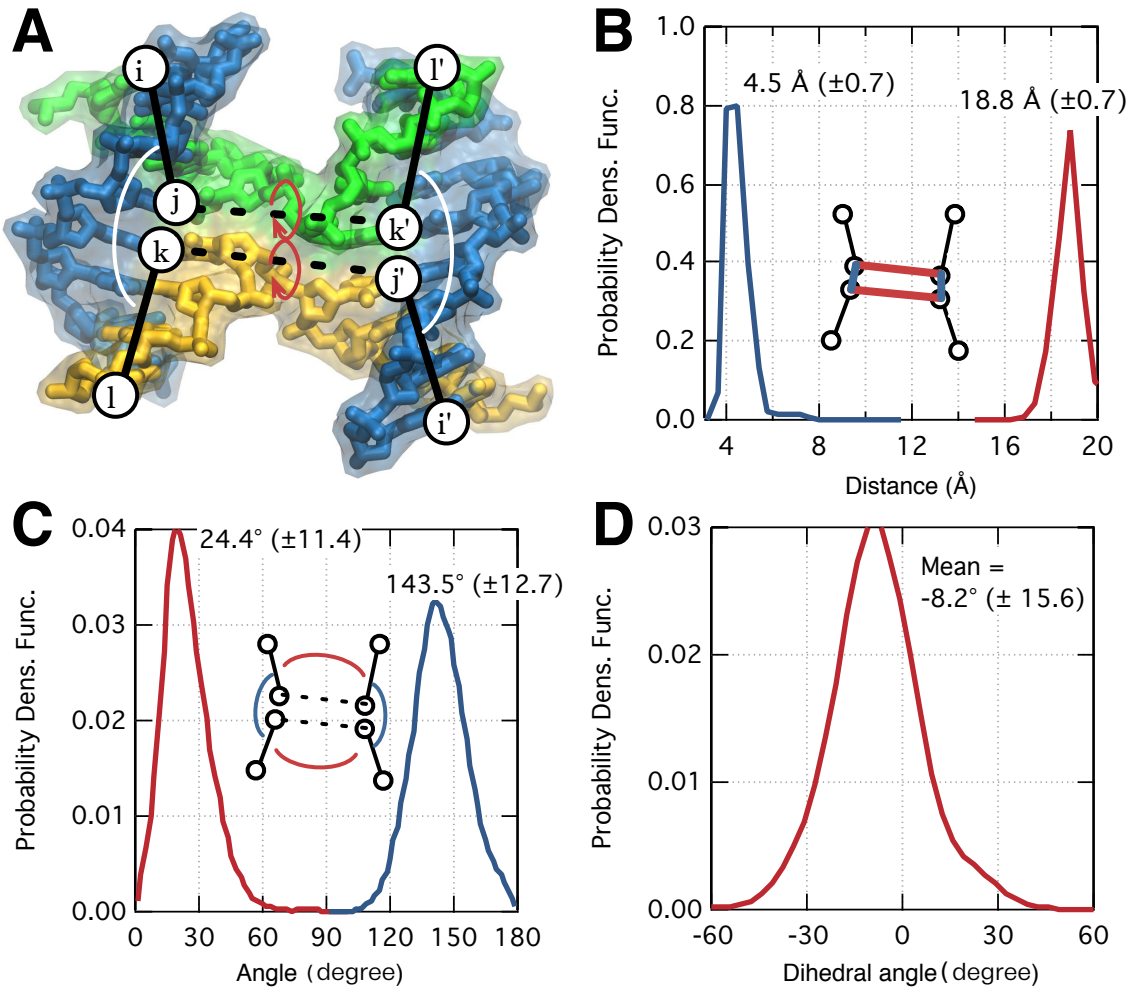

Fig. S8. The structure of Holliday junctions in the SQ system. (A) A typical conformation of a Holliday junction in DNA origami object. The two crossover staple strands are shown in green and orange; the fragments of the scaffold strand are shown in blue. Points i, i', j, j', k, k', l and l' indicate the locations of the centers of mass of the base pairs at the junction (j, j', k, k') and three base-pair away from the junction, (i, i', l, l'). (B) The distributions of distances between base pairs at the junction. Blue corresponds to the intra-helical distance $j-k$ (or $j'-k'$); red corresponds to the inter-helical distances $j-k'$ (or $k-j'$). (C) The bending angle of the helices at the junction (blue) and the angle between the helices at the junction (red). (D) The distribution of the dihedral angle $i-j-k-l$ (or $i'-j'-k'-l'$). All distributions were obtained by averaging over the last 60 ns of the SQ trajectory and over all junctions in the structure. In panels B–D, mean and standard deviation of each distribution function are shown in numbers.

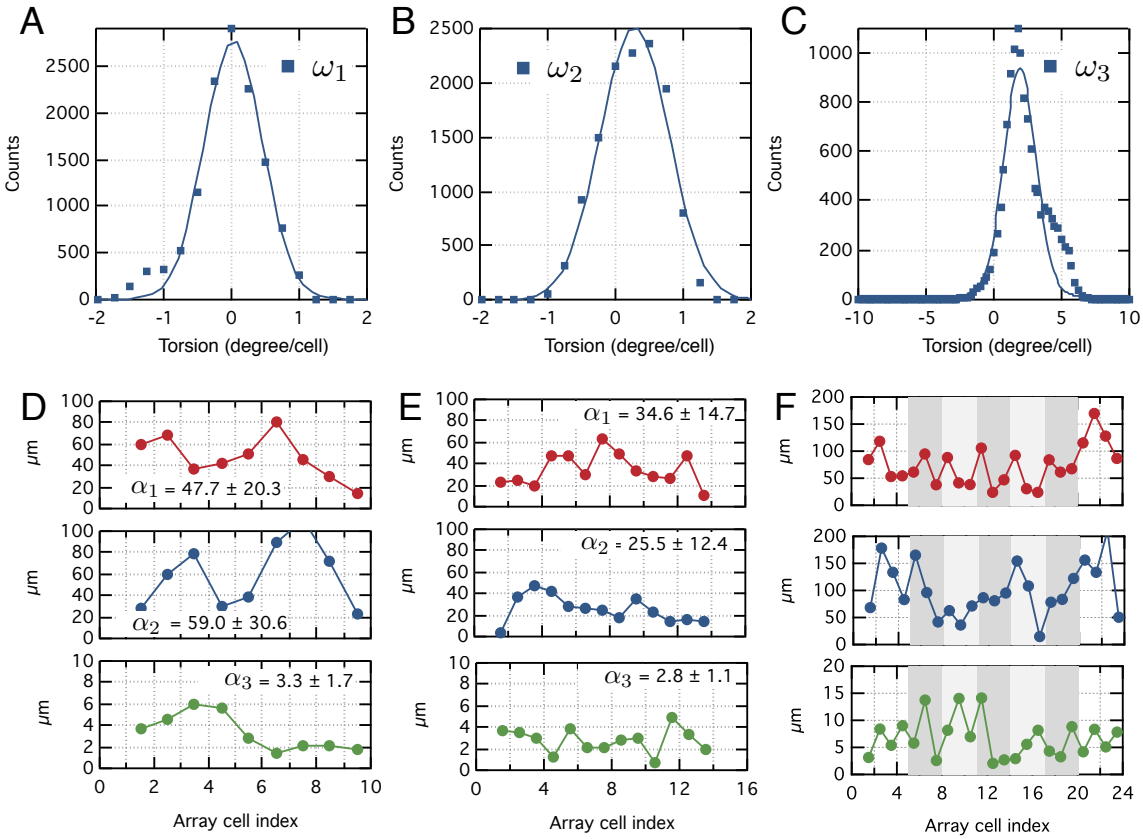

Fig. S9. (A–C) Representative distributions of generalized torsions, ω_1, ω_2, and ω_3. Histograms of torsions ω_1 (A), ω_2 (B), and ω_3 (C) between array cells 4 and 5 of the HC system (symbols). Gaussian fits to the histograms are shown as solid lines. (D–F) Bending ($\alpha_{1,2}$) and twist (α_3) moduli in the HC (D), SQ (E), and HC-90° (F) structures as a function of the array cell index.

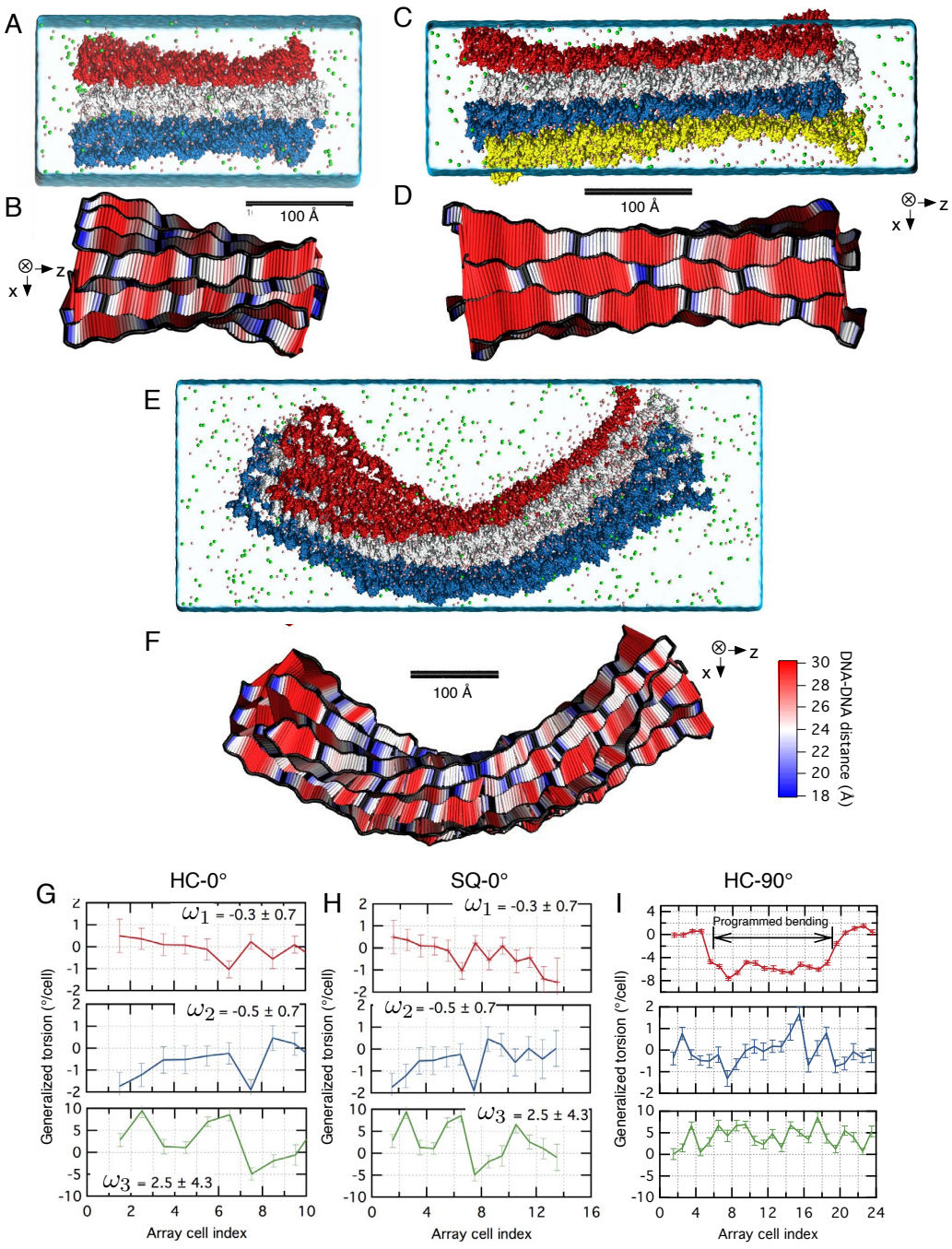

Fig. S10. Structural and mechanical properties of the DNA origami systems simulated using the AMBER99bsc0 force field. (A–F) The conformations of HC-AMBER, SQ-AMBER, and HC-90°-AMBER systems at the end of the production runs are shown in panels A, C, and E, respectively; the same conformations are also shown in a chickenwire represenation in panels B, D, and F, respectively. In panels A, C, and E, DNA origami is shown as a molecule surface with each layer of DNA drawn in the same color; Mg^{2+} and Cl^- ions are shown as pink and green spheres, respectively; the semi-transparent blue surfaces depict the water box. (G–I) Generalized torsions, $\omega_{1,2,3}$ (from top to bottom), as a function of the array cell index in the HC-AMBER (G), SQ-AMBER (H), and HC-90°-AMBER (I) systems.